

Discovery prospects of a singly-charged scalar at μ TRISTAN

Joseph George^{1,2*}, Nobuchika Okada^{3†}, Dibyashree Sengupta^{4,5‡}, Sudhir K. Vempati^{6§}

¹*Department of Physics, Indian Institute of Science Education and Research Pune, Pune 411008, India*

² *National Centre for Nuclear Research, Warsaw 02-093, Poland*

³*Department of Physics and Astronomy, University of Alabama, Tuscaloosa, Alabama 35487, USA*

⁴*INFN, Sezione di Roma, c/o Dip. di Fisica, Sapienza Università di Roma, Piazzale Aldo Moro 2, I-00185 Rome, Italy*

⁵*Department of Physics, University of Cyprus, P.O. Box 20537, 1678 Nicosia, Cyprus*

⁶*Centre for High Energy Physics, Indian Institute of Science, Bangalore 560012, India*

Abstract

In this article, we study the associated production of a singly-charged (Δ^+) scalar along with a W^+ boson in the newly proposed $\mu^+\mu^+$ collider (also known as μ TRISTAN) at $\sqrt{s} = 2$ TeV. Such a singly-charged scalar is naturally accommodated in an extremely well-motivated neutrino mass model, namely, the Type-II seesaw model. This model, beside providing a viable explanation of neutrino mass generation, also allows for lepton flavor violating (LFV) processes. Since LFV processes are not allowed in the Standard Model (SM), we focus on the discovery prospect of the singly-charged scalar in the Type-II seesaw model at μ TRISTAN through a LFV process, owing to the advantage of this process being free of any SM background. Additionally, this article also proposes a method to indicate if the underlying theory follows a Normal or an Inverted hierarchy depending on the distribution of lepton flavors in the final state.

*E-mail: joseph.george@ncbj.gov.pl

†E-mail: okadan@ua.edu

‡E-mail: sengupta.dibyashree@ucy.ac.cy

§E-mail: vempati@iisc.ac.in

1 Introduction

The Standard Model (SM), till date, is the most successful theory of nature which attained its peak with the discovery of the Higgs boson in 2012 at ATLAS and CMS [1, 2]. Despite such massive success of the SM, it cannot explain various natural phenomena such as : 1. Neutrino mass generation mechanism [3, 4], 2. Higgs mass instability in the electroweak sector [5–7], 3. Matter-Antimatter assymmetry [8], 4. the Strong CP problem [9–11] and several others. Such drawbacks of the SM motivate the existence of Beyond Standard Model (BSM) scenarios.

An extremely well-motivated BSM scenario is the Type-II seesaw scenario [12–15] which not only provides a valid explanation for neutrino mass generation mechanism but also allows for LFV processes which the SM does not accommodate. Therefore, it is highly lucrative to look for the exotic BSM particles which can vouch for the existence of the Type-II seesaw model through a LFV process since such a process will have no relevant SM background and hence will be extremely clean. All existing collider constraints on the Type-II seesaw model can be found in Ref. [16, 17]. Ref. [18, 19] summarizes the LFV constraints.

Lepton colliders are extremely advantageous for looking into LFV processes as they provide a much cleaner environment than hadron colliders. Additionally, since leptons are fundamental particles, the entire beam energy is available for the hard collision. Whereas, in a hadron collider such as the LHC, only a fraction of the proton-beam energy that is carried by the colliding partons is available for collision. Therefore, a higher physics reach is obtained in lepton colliders. Lepton colliders are constructed by colliding Electrons or Muons. However, since Muons are heavier than Electrons, colliding Muons leads to much smaller loss of energy due to synchrotron radiations as compared to colliding Electrons. Thanks to the huge development in technology we can now solve several technical difficulties that had been hindering the operation of a $\mu^+\mu^-$ collider, thereby, making the $\mu^+\mu^-$ collider gain huge interest in the community in recent years [20–24]. Numerous studies have been performed showing the huge prospect of the $\mu^+\mu^-$ collider in search of new physics [25].

However, in this article we concentrate on a slightly different setup, namely the μ TRISTAN [26] which plans on operating as a μ^+e^- collider at $\sqrt{s} = 346$ GeV and a $\mu^+\mu^+$ collider at $\sqrt{s} = 2$ TeV and higher [27]. We study our signature of choice in the $\mu^+\mu^+$ mode of the μ TRISTAN. Apparently the $\mu^+\mu^+$ collider is quite convenient to build, thanks to the cooling technology developed at J-PARC [28]. Several studies have been performed showing the discovery prospects of new physics in μ TRISTAN [29–37]. In this article we intend to look for the singly-charged scalar that can be naturally accommodated in the Type-II seesaw model via its associated production along with a W^+ boson in the $\mu^+\mu^+$ collider at $\sqrt{s} = 2$ TeV, followed by its decay in channels such that our signature of interest is a LFV

process. Following the discovery prospects of the singly-charged scalar, we also propose a technique to identify whether the underlying theory respects Normal hierarchy or Inverted hierarchy depending on the flavors of the lepton in the final state.

The rest of the article is organized as follows. In Sec. 2, we discuss in detail the Type-II seesaw model. In Sec. 3, we present our signature of interest and motivation behind choosing this signal along with the benchmark points. Sec. 4 discusses the signal analysis and mass reach of the singly charged scalar, while Sec. 5 presents the technique to distinguish between the Normal and Inverted hierarchy. Finally in Sec. 6 we provide the summary and outlook.

2 Type-II seesaw model

In Type-II seesaw scenario [12–15] the SM particle spectrum is augmented with a $SU(2)_L$ triplet scalar $\Delta = (\Delta^{++}, \Delta^+, \Delta^0)$ with hypercharge $Y_\Delta = 1$. Therefore, the scalar sector of this BSM scenario consists of the following:

$$\Delta = \begin{pmatrix} \Delta^+/\sqrt{2} & \Delta^{++} \\ \Delta^0 & -\Delta^+/\sqrt{2} \end{pmatrix}, \quad \Phi = \begin{pmatrix} \phi^+ \\ \phi^0 \end{pmatrix}, \quad (2.1)$$

where Φ is the SM Higgs doublet.

This additional scalar Δ , being charged under $SU(2)_L$, interacts with the SM gauge sector and also has Yukawa interaction terms with the SM lepton doublets. Therefore, the Lagrangian terms that arise due to this additional scalar beside the SM Lagrangian are:

$$\mathcal{L}_{BSM} = Tr[(D_\mu \Delta)^\dagger D^\mu \Delta] + (Y_{\alpha\beta} \overline{L^\alpha} (i\sigma_2) \Delta L^\beta + h.c.) - V(\Delta, \Phi), \quad (2.2)$$

where the first term with covariant derivative D_μ denotes the interaction between Δ and the SM gauge sector where D_μ is given by

$$D_\mu \Delta = \partial_\mu \Delta - \frac{i}{2} g \left(\sum_{k=1,2,3} W_\mu^k [\sigma_k \Delta - \Delta \sigma_k] \right) - ig' y_\Delta B_\mu \Delta, \quad (2.3)$$

where σ_k are the Pauli spin matrices, g and g' are the gauge couplings of Δ with $SU(2)_L$ and $U(1)_Y$ SM gauge bosons, respectively, and y_Δ is the hypercharge of Δ which is postulated to be 1.

The second term in Eqn. (2.2) denotes the Yukawa interaction between Δ and the SM left-handed weak lepton doublets denoted by L^α and L^β where α and β are the flavor indices. The generic form of the SM left-handed weak lepton doublet is given by

$$L = \begin{pmatrix} \nu_e \\ e^- \end{pmatrix}_L \quad (2.4)$$

The term $V(\Delta, \Phi)$ in Eqn. (2.2) is the scalar potential which can be written as:

$$V(\Delta, \Phi) = -m_\Phi^2 \Phi^\dagger \Phi + \frac{\lambda}{4} (\Phi^\dagger \Phi)^2 + M_\Delta^2 \text{Tr}[\Delta^\dagger \Delta] + \lambda_1 [\text{Tr} \Delta^\dagger \Delta]^2 + \lambda_2 \text{Tr}[\Delta^\dagger \Delta]^2 + [\mu \Phi^T i \sigma_2 \Delta^\dagger \Phi + h.c.] + \lambda_3 (\Phi^\dagger \Phi) \text{Tr}[\Delta^\dagger \Delta] + \lambda_4 \Phi^\dagger \Delta \Delta^\dagger \Phi, \quad (2.5)$$

where μ and λ_i ($i = 1, 2, 3, 4$) are the relevant couplings among the SM and BSM scalars.

On minimizing the scalar potential in Eqn. (2.5) one can obtain a VEV of Δ^0 (denoted by v_Δ) in Eqn. (2.2) and with the SM Higgs VEV (denoted by v), one can obtain the neutrino mass as :

$$m_\nu = \sqrt{2} Y v_\Delta, \quad (2.6)$$

where $v_\Delta \sim \mu v^2 / (\sqrt{2} M_\Delta^2)$.

The neutrino mass matrix can be diagonalized using the PMNS matrix denoted by U_{PMNS} as follows:

$$m_\nu^{diag} = \text{Diag}[m_{\nu_1}, m_{\nu_2}, m_{\nu_3}] = U_{PMNS}^* m_\nu U_{PMNS}^\dagger. \quad (2.7)$$

The neutrino mass hierarchy can either respect normal ordering (i.e., ν_1 is the lightest) or inverted ordering (i.e., ν_3 is the lightest). Here we study both cases and propose a method to distinguish between these two cases depending on the phenomenological manifestation at the $\mu^+ \mu^+$ Collider.

After the electroweak symmetry breaking, this BSM scenario yields seven physical states of definite mass in the scalar sector. These states are denoted by $H^{\pm\pm}$, H^\pm , H^0 , A^0 and h where h is the SM Higgs boson, A^0 is a pseudoscalar, H^0 is the electrically-neutral heavy scalar, and $H^{\pm\pm}$ and H^\pm are electrically-charged heavy scalars.

From Eqn. (2.7), one can deduce that in order to obtain a small mass for the neutrino as supported by experiments, v_Δ must be quite small. In the simplest type-II seesaw model [12–15], v_Δ is bounded by the electroweak ρ parameter constraining $v_\Delta \lesssim 3$ GeV [38]. In the limit $v_\Delta \ll v$, the mass eigen states of the scalar triplet appear as :

$$m_{H^{++}} \sim m_{\Delta^{++}}, m_{H^+} \sim m_{\Delta^+}, m_{H^0} \sim \text{Re}[m_{\Delta^0}], m_{A^0} \sim \text{Im}[m_{\Delta^0}] \\ m_{H^0}^2 \approx m_{A^0}^2 \approx m_{H^+}^2 + \frac{\lambda_4}{4} v^2 \approx m_{H^{++}}^2 + \frac{\lambda_4}{2} v^2. \quad (2.8)$$

Depending on the value and sign of λ_4 , the mass ordering of the scalar triplets can be :

- i) $\lambda_4 = 0$: $m_{H^0}^2 = m_{A^0}^2 = m_{H^+}^2 = m_{H^{++}}^2$.
- ii) $\lambda_4 < 0$: $m_{H^0}^2 = m_{A^0}^2 < m_{H^+}^2 < m_{H^{++}}^2$.
- iii) $\lambda_4 > 0$: $m_{H^0}^2 = m_{A^0}^2 > m_{H^+}^2 > m_{H^{++}}^2$.

In this article, we choose the second case with the mass hierarchy $m_{H^0}^2 = m_{A^0}^2 < m_{H^+}^2 < m_{H^{++}}^2$ with the mass difference of $\sim 1\text{-}2$ GeV. In the rest of the article, we denote the physical states $H^{\pm\pm}$, H^\pm and H^0 by $\Delta^{\pm\pm}$, Δ^\pm and Δ^0 , respectively.

3 Signature of interest and Benchmark points

Several studies have previously been performed to look for the doubly-charged scalar Δ^{++} and electrically-neutral scalar Δ^0 in the Muon collider [25, 39] as well as the $\mu^+\mu^+$ mode of the μ TRISTAN [33–36]. A comparative study of the doubly-charged scalar Δ^{++} at the Muon collider and the $\mu^+\mu^+$ mode of the μ TRISTAN for the chosen benchmark points has been shown in Appendix A and Appendix B. However, the discovery prospects of the singly-charged scalar Δ^+ have not yet received much deserved attention. Therefore, here in this article we study the associated production of Δ^+ along with the W^+ boson in the $\mu^+\mu^+$ mode of the μ TRISTAN, followed by hadronic decay of the W^+ boson and leptonic decay of Δ^+ . This associated production of Δ^+ and W^+ involves two types of contribution: (i) mediated by a virtual Δ^{++} in s-channel and (ii) mediated by exchange of a ν_l in t-channel. The generic Feynman diagrams of these processes are shown in Fig. 1a and Fig 1b, respectively.

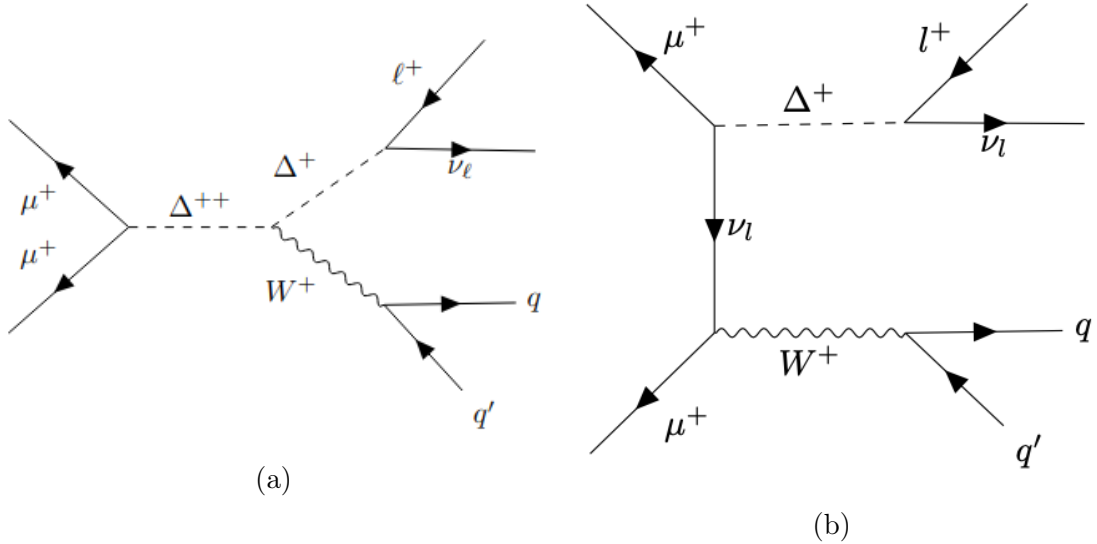


Figure 1: Generic Feynman diagram for signal

If the lepton arising from the decay of the Δ^+ is a μ^+ , then the process in Fig. 1 has a sizeable SM background ≈ 0.92 pb. However, if one considers the final state lepton to be e^+ or τ^+ , then there is no relevant SM background as in order to generate such a process, lepton flavor violation is needed which the SM does not accommodate. Hence, finally our chosen signature of interest consists of only e^+ or τ^+ as the final state charged leptons as shown in Fig. 2. This choice helps to get rid of any SM background as discussed above.

Benchmark points:

As benchmark points, we consider two values of the lightest neutrino mass : 0.05 eV and 0.001 eV. The VEV of Δ^0 , denoted as v_Δ , is fixed at 10^{-9} GeV as at such a small value of

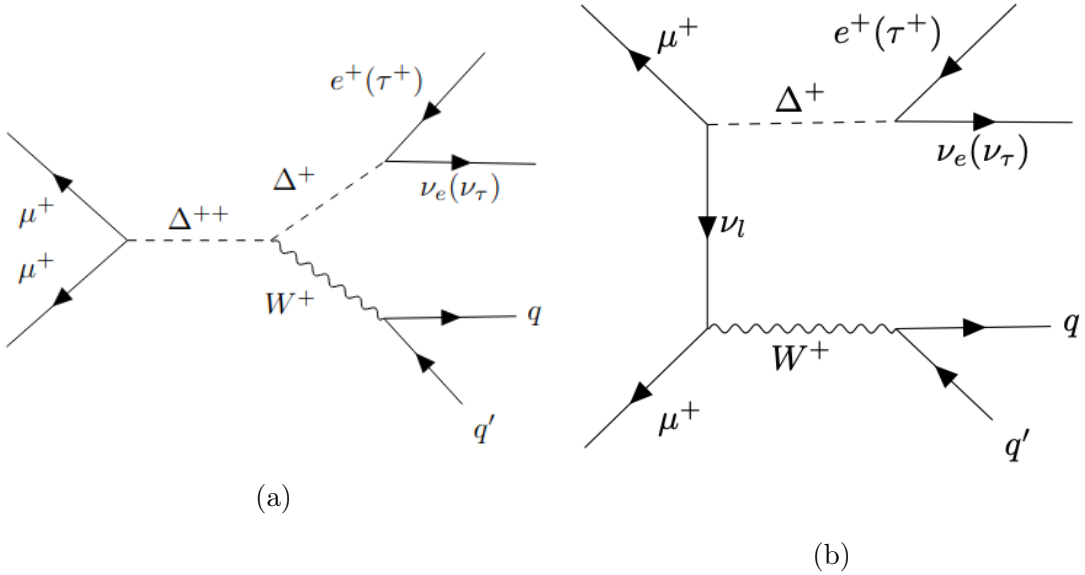


Figure 2: Feynman diagram for lepton flavor violating (LFV) signal processes chosen to get rid of any SM background.

v_Δ , Δ^+ primarily decays to leptons. The analysis is performed by varying the mass of Δ^+ in between 101 GeV and 1901 GeV at an interval of 100 GeV for both Normal and Inverted Hierarchy at $\sqrt{s} = 2$ TeV. The benchmark points for $m_{\Delta^+} = 101, 301, 501, 1001, 1501$ and 1901 GeV and the lightest neutrino mass : 0.05 eV and 0.001 eV are shown in Table. I and Table. II, respectively. The production cross-section for our signal of interest is shown in Fig. 3 which exhibits a fall and rise behavior with increase in mass of Δ^+ . This typical behavior of the cross-section for our signal of interest is due to the contribution from Fig. 2b as discussed in detail in Appendix C. The branching ratios of Δ^+ in different channels are shown for Normal and Inverted Hierarchy in Fig. 4a and Fig. 4b, respectively. The branching ratios of Δ^+ do not change with change in its mass, as can be seen in Fig. 4. Although for Normal hierarchy the branching ratio for Δ^+ to decay into μ^+ is higher than that for decaying into e^+ or τ^+ for a particular value of lightest neutrino mass, as evident from Fig: 4a, we consider the decay of Δ^+ to e^+ and τ^+ only, as then the process is absolutely free of SM background, as mentioned earlier, although at a cost of losing a reasonable number of signal events. But since the surviving events don't have any SM background, those small number of events are sufficient to yield 5σ significance up to a certain mass of Δ^+ which will be discussed in detail in Sec. 4. For Inverted Hierarchy, however, the branching ratio for Δ^+ to decay into μ^+ is smaller than that for decaying into e^+ or τ^+ . Therefore, for Inverted Hierarchy, selecting the decay of Δ^+ to e^+ and τ^+ only makes the process free of SM background without much loss of signal events. Although the branching ratios of Δ^+ do not change with its mass, they do change with change in the mass of the

lightest neutrino, as evident from Fig 5.

Masses [GeV]			Normal Hierarchy						Inverted Hierarchy					
m_{Δ^0}	m_{Δ^+}	$m_{\Delta^{++}}$	Γ_{Δ^0}	Γ_{Δ^+}	$\Gamma_{\Delta^{++}}$	$\sigma_{Production}$	σ	S/\sqrt{S}	Γ_{Δ^0}	Γ_{Δ^+}	$\Gamma_{\Delta^{++}}$	$\sigma_{Production}$	σ	S/\sqrt{S}
100	101	103	0.02	0.0202	0.0206	0.01474	0.0055	12.845	0.0247	0.0249	0.0254	0.01324	0.006	13.42
300	301	303	0.0601	0.0603	0.0607	0.01156	0.0043	11.358	0.0742	0.0744	0.0749	0.01039	0.0046	11.75
500	501	503	0.1002	0.1004	0.1008	0.01038	0.004	10.95	0.1236	0.1239	0.1243	0.00933	0.0041	11.09
1000	1001	1003	0.2004	0.2006	0.201	0.01047	0.004	10.95	0.2472	0.2475	0.248	0.009413	0.0041	11.09
1500	1501	1503	0.3006	0.3008	0.3012	0.01526	0.0057	13.08	0.3708	0.3711	0.3716	0.01371	0.006	13.42
1900	1901	1903	0.3808	0.381	0.3814	0.00563	0.0021	7.94	0.4697	0.47	0.4704	0.00506	0.0022	8.12

Table I: Benchmark Points for Normal and Inverted Hierarchy at $v_{\Delta} = 10^{-9}$ GeV and lightest neutrino mass = 0.05 eV. The cross-sections listed here are for the processes before and after decay of Δ^+ and W^+ (as in Fig. 2) at $\sqrt{s} = 2$ TeV. The significance listed here is at Integrated Luminosity $\mathcal{L} = 30 \text{ fb}^{-1}$. All the masses and decay widths(Γ) are in units of GeV and the cross-sections $\sigma_{Production}$ and σ are in units of pb.

Masses [GeV]			Normal Hierarchy						Inverted Hierarchy					
m_{Δ^0}	m_{Δ^+}	$m_{\Delta^{++}}$	Γ_{Δ^0}	Γ_{Δ^+}	$\Gamma_{\Delta^{++}}$	$\sigma_{Production}$	σ	S/\sqrt{S}	Γ_{Δ^0}	Γ_{Δ^+}	$\Gamma_{\Delta^{++}}$	$\sigma_{Production}$	σ	S/\sqrt{S}
100	101	103	$5.13 \cdot 10^{-3}$	$5.18 \cdot 10^{-3}$	$5.28 \cdot 10^{-3}$	0.003614	0.001	5.48	$9.806 \cdot 10^{-3}$	$9.902 \cdot 10^{-3}$	$1.01 \cdot 10^{-2}$	0.001833	0.0009	5.2
300	301	303	$1.538 \cdot 10^{-2}$	$1.543 \cdot 10^{-2}$	$1.553 \cdot 10^{-2}$	0.002834	0.0008	4.9	$2.942 \cdot 10^{-2}$	$2.952 \cdot 10^{-2}$	$2.971 \cdot 10^{-2}$	0.001437	0.0007	4.6
500	501	503	$2.563 \cdot 10^{-2}$	$2.568 \cdot 10^{-2}$	$2.58 \cdot 10^{-2}$	0.002546	0.0007	4.6	$4.903 \cdot 10^{-2}$	$4.913 \cdot 10^{-2}$	$4.932 \cdot 10^{-2}$	0.001291	0.0006	4.2
1000	1001	1003	$5.126 \cdot 10^{-2}$	$5.132 \cdot 10^{-2}$	$5.142 \cdot 10^{-2}$	0.002569	0.0007	4.6	$9.806 \cdot 10^{-2}$	$9.816 \cdot 10^{-2}$	$9.836 \cdot 10^{-2}$	0.001303	0.00063	4.3
1500	1501	1503	$7.69 \cdot 10^{-2}$	$7.695 \cdot 10^{-2}$	$7.705 \cdot 10^{-2}$	0.003742	0.001	5.48	$1.471 \cdot 10^{-1}$	$1.472 \cdot 10^{-1}$	$1.474 \cdot 10^{-1}$	0.001898	0.001	5.48
1900	1901	1903	$9.741 \cdot 10^{-2}$	$9.746 \cdot 10^{-2}$	$9.756 \cdot 10^{-2}$	0.001381	0.0004	3.5	$1.863 \cdot 10^{-1}$	$1.864 \cdot 10^{-1}$	$1.866 \cdot 10^{-1}$	0.0007004	0.00034	3.2

Table II: Benchmark Points for Normal and Inverted Hierarchy at $v_{\Delta} = 10^{-9}$ GeV and lightest neutrino mass = 0.001 eV. The cross-sections listed here are for the processes before and after decay of Δ^+ and W^+ (as in Fig. 2) at $\sqrt{s} = 2$ TeV. The significance listed here is at Integrated Luminosity $\mathcal{L} = 30 \text{ fb}^{-1}$. All the masses and decay widths(Γ) are in units of GeV and the cross-sections $\sigma_{Production}$ and σ are in units of pb.

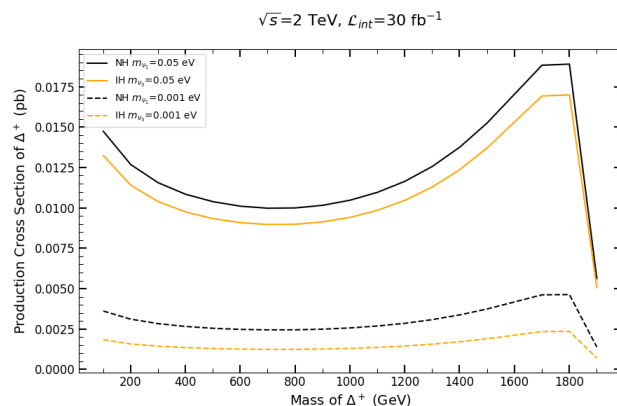


Figure 3: Cross-Section for the process $\mu^+ \mu^+ \rightarrow \Delta^+ W^+$ for masses of Δ^+ varying between 101 and 1901 GeV.

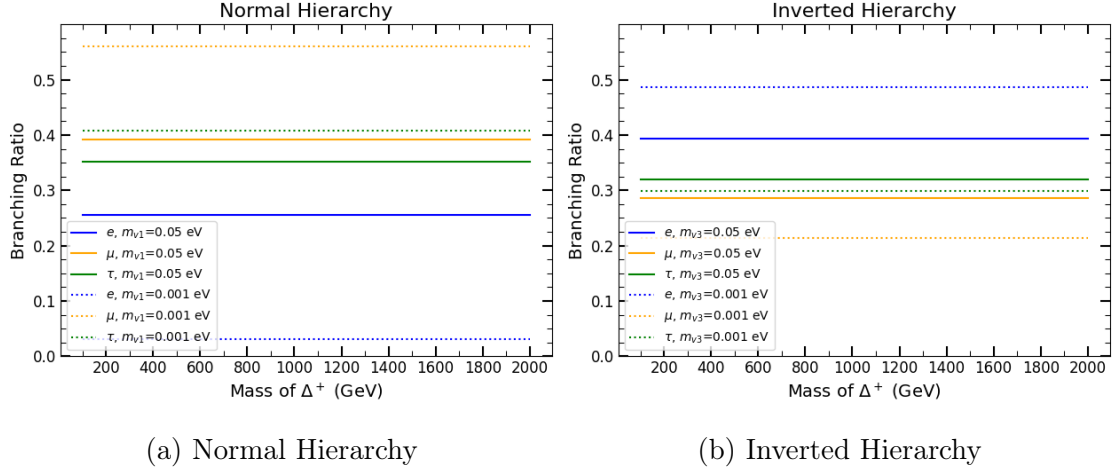


Figure 4: Branching Ratio of Δ^+ for masses of Δ^+ varying between 101 and 1901 GeV.

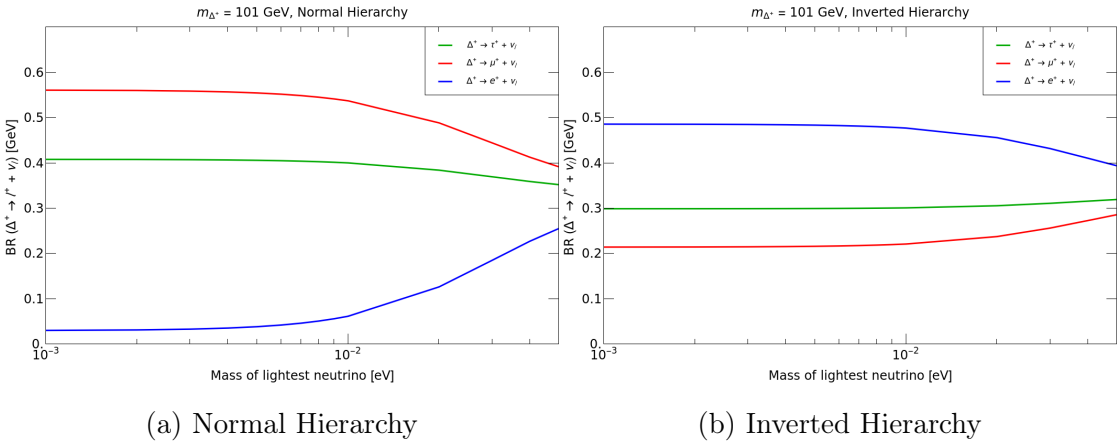


Figure 5: Branching Ratio of Δ^+ for masses of the lightest neutrino varying between 0.05 and 0.001 eV for a fixed $m_{\Delta^+} = 101$ GeV.

4 Signal analysis and Mass reach of Δ^+

All benchmark points have been generated using the UFO model [40] and simulated using MADGRAPH [41] followed by showering in PYTHIA [42] and detector level analysis in DELPHES [43] using the default Muon collider delphes card. The total cross-section of the full process, as in Fig. 2, is calculated at $\sqrt{s} = 2$ TeV and shown in Fig. 6a. Since the process involves lepton flavor violation, it is a noble signature with absolutely zero SM background. Therefore, the significance for Fig. 2 can be calculated as

$$\text{significance} = S/\sqrt{S}^1$$

¹For simplicity, Gaussian distribution has been used here to calculate the significance. In experimental analyses, Poisson statistics should be used to compute the statistical significance more accurately, particularly in regimes with limited background events. At the limit $B \rightarrow 0$, Poisson statistics will yield the significance $\sim \sqrt{2S\ln(1/B)}$, where B is the number of background events and S is the number of signal events. Although theoretically, one would expect absolutely no background events for the signature

where S is the number of signal events which is calculated as

$$S = \sigma \times \mathcal{L}_{int}, \quad (4.9)$$

where σ is the cross-section, which is shown in Fig. 6a and \mathcal{L}_{int} is the integrated Luminosity which has been considered to be 30 fb^{-1} .

The significance for all the benchmark points have been shown in Fig. 6b. In Fig. 6a and Fig. 6b, the solid curves are for the points with mass of lightest neutrino = 0.05 eV and the dashed curves are for the points with mass of lightest neutrino = 0.001 eV. The black curves denote Normal Hierarchy and the orange curves denote Inverted Hierarchy. The horizontal red and blue lines in Fig. 6a and Fig. 6b denote significance of 5σ and 95% CL, respectively. As can be noted from Fig. 6, all the points for $m_{\nu_{lightest}} = 0.05 \text{ eV}$ and for both Normal and Inverted Hierarchy have significance above 5σ while for $m_{\nu_{lightest}} = 0.001 \text{ eV}$, all the points have significance above 95% CL but not all of them have significance above 5σ . For Normal hierarchy points with $m_{\nu_{lightest}} = 0.001 \text{ eV}$ and $m_{\Delta^+} \lesssim 141 \text{ GeV}$ and $1412 \lesssim m_{\Delta^+} \lesssim 1832 \text{ GeV}$ have significance above 5σ and for Inverted hierarchy points with $m_{\nu_{lightest}} = 0.001 \text{ eV}$ and $m_{\Delta^+} \lesssim 208 \text{ GeV}$ and $1306 \lesssim m_{\Delta^+} \lesssim 1841 \text{ GeV}$ have significance above 5σ , as evident from Fig. 6. One should note that apart from slight difference in the values of cross-section and significance in between Normal and Inverted Hierarchy, there is not much difference between these two cases. The shapes of the curves, as shown in Fig. 6, are same for both Normal and Inverted Hierarchy. Therefore, using these curves one cannot identify whether the underlying mechanism is Normal or Inverted Hierarchy. However, the flavors in the final-state leptons will vary a lot for these two cases and hence can be used to differentiate between Normal and Inverted Hierarchy, as discussed in detail in the next Section.

5 Differentiating Normal Hierarchy from Inverted Hierarchy

As discussed in Sec. 4, it is possible to obtain a significant amount of cross-section for our signature of interest for both Normal and Inverted Hierarchies in the $\mu^+ \mu^+$ collider, enough to confirm discovery of a singly-charged scalar Δ^+ . However, the results obtained in Fig. 6 are not sufficient to identify whether the underlying theory respects Normal Hierarchy or Inverted Hierarchy. This important fact can be ensured by the distribution of final state

considered here, in practice, a non-zero background will arise experimentally due to uncertainties. Such a background can then be incorporated into this expression to obtain a finite and physically meaningful significance. This approach generally yields a higher significance than that obtained here using Gaussian approximations. Consequently, our calculation is conservative: an experimental determination of the significance is expected to be equal to or greater than our result, but not smaller.

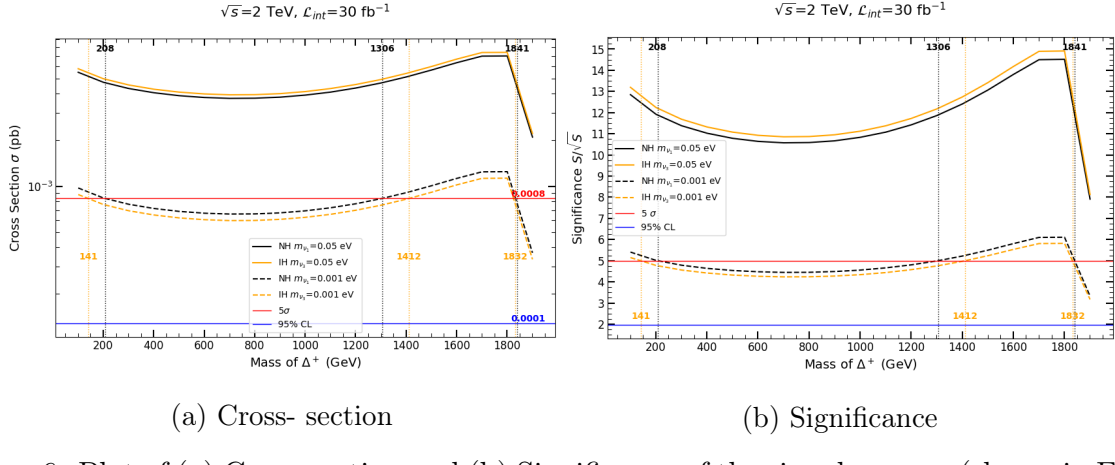


Figure 6: Plot of (a) Cross-section and (b) Significance of the signal process (shown in Fig. 2) vs. m_{Δ^+} showing the 5σ and 95% CL level by the horizontal red and blue line respectively.

Electrons and Taus originating from the decay of Δ^+ .

The distribution of Electrons and Taus in the final state for Normal and Inverted Hierarchy are shown in Fig. 7 and Fig. 8, respectively for benchmark points with the lightest neutrino mass $m_{\nu_{lightest}} = 0.05 \text{ eV}$ and $m_{\Delta^+} = 101, 501, 1001, 1501, 1901 \text{ GeV}$. Similar plots for benchmark points with the lightest neutrino mass $m_{\nu_{lightest}} = 0.001 \text{ eV}$ and $m_{\Delta^+} = 101, 501, 1001, 1501, 1901 \text{ GeV}$ are shown in Fig. 9 and Fig. 10 for Normal and Inverted Hierarchy, respectively. Although the signature of interest should ideally yield exactly one charged lepton (either e^+ or τ^+), there are many events with no e^+ or τ^+ in the final state as evident in Fig. 7 - Fig. 10. This is because for a huge number of events the final state charged lepton escapes detection for lying outside the range of pseudorapidity that the detector can cover and hence is highly dependent on the detector design. However, this situation improves as m_{Δ^+} increases and more and more events yield detectable charged lepton in the final state. One might notice there are some events which have 2 charged Electrons/taus in the final state but these events arise due to misidentification of a jet as a lepton. However, one must note that these events are negligibly small in number.

In order to identify whether the theory respects Normal or Inverted hierarchy, one must compare the distribution of final state Electrons and Taus. We compare the distribution of Electrons and Taus in the final state for Normal and Inverted hierarchies in Fig. 11a and Fig. 11b, respectively, for a particular benchmark point characterized with $m_{\nu_{lightest}} = 0.05 \text{ eV}$ and $m_{\Delta^+} = 101 \text{ GeV}$. Similar plots for two other masses of $\Delta^+ = 1001 \text{ GeV}$ and 1901 GeV have been shown in Fig. 12 and Fig. 13, respectively. While one compares the Electron and Tau distribution for a particular benchmark point with a characteristic hierarchy, one must be careful to compare the relevant events i.e., the events which have exactly one charged lepton in the final state. Therefore, comparing such relevant events in Fig. 11, Fig. 12 and Fig. 13 one would expect that in case of Normal hierarchy there would be more events with

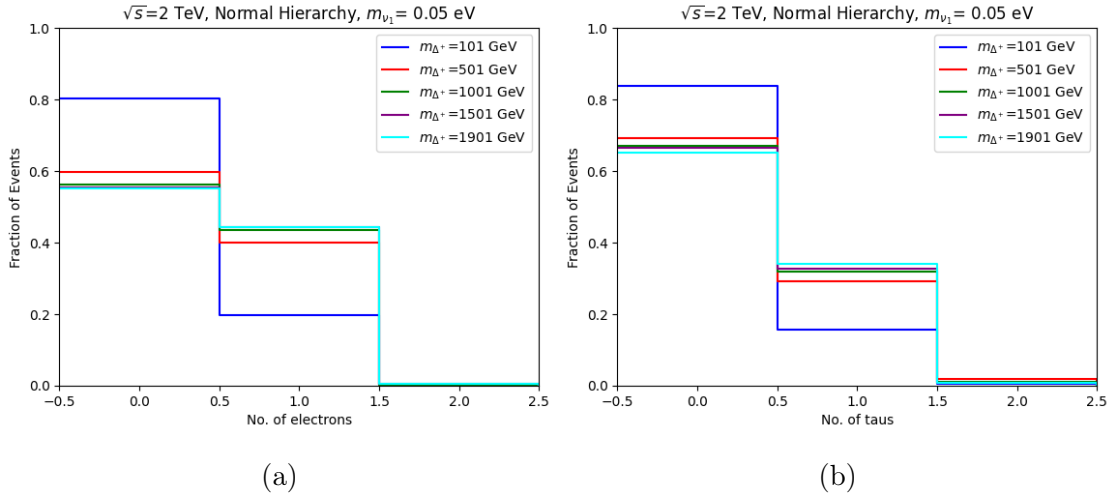


Figure 7: Distribution for a) Electrons in the final state and b) Taus in the final state for $m_{\nu_1} = 0.05 \text{ eV}$ assuming Normal Hierarchy

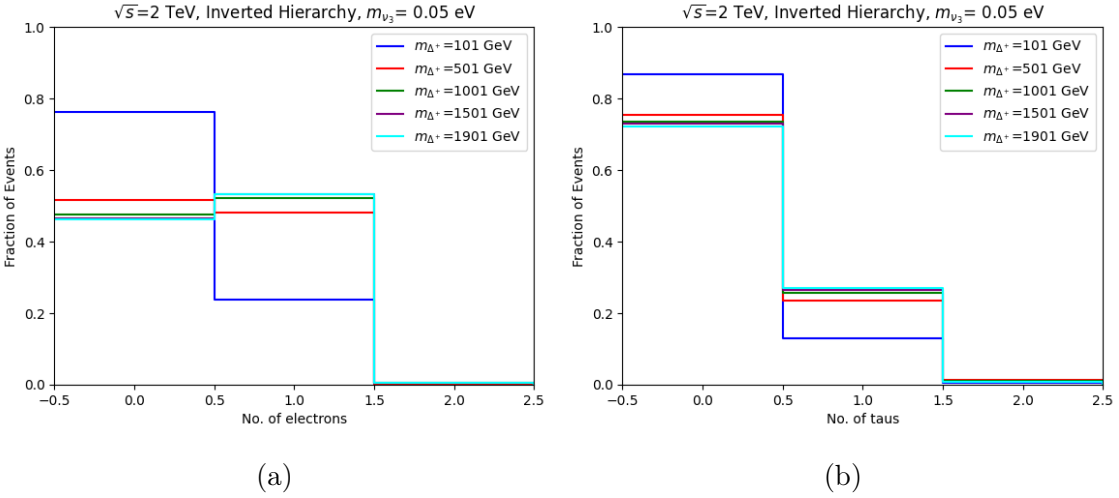


Figure 8: Distribution for a) Electrons in the final state and b) Taus in the final state for $m_{\nu_3} = 0.05 \text{ eV}$ assuming Inverted Hierarchy

Taus in the final state than with final state Electrons while for Inverted hierarchy there would be more events with Electrons in the final state than with final state Taus, as evident from Fig. 4. However, for bm points with lightest neutrino mass = 0.05 eV, there are always more events with Electrons than Taus in the final state irrespective of the underlying hierarchy. The difference between the hierarchies are not observable for bm points with lightest neutrino mass = 0.05 eV because for such high mass of the lightest neutrino the difference in the branching ratios of Δ^+ in different leptonic channels is quite small, as evident from Fig. 5. The difference between the hierarchies for massive lightest neutrino can be improved by modifying the detector structure and taking into consideration several other factors such as uncertainties, response functions etc. However, these factors are not yet known and hence

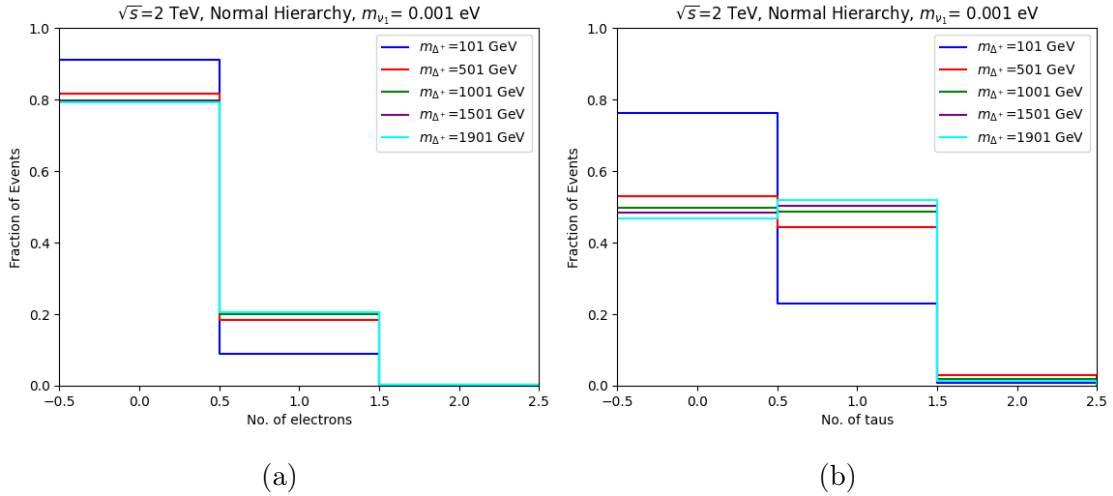


Figure 9: Distribution for a) Electrons in the final state and b) Taus in the final state for $m_{\nu_1} = 0.001 \text{ eV}$ assuming Normal Hierarchy

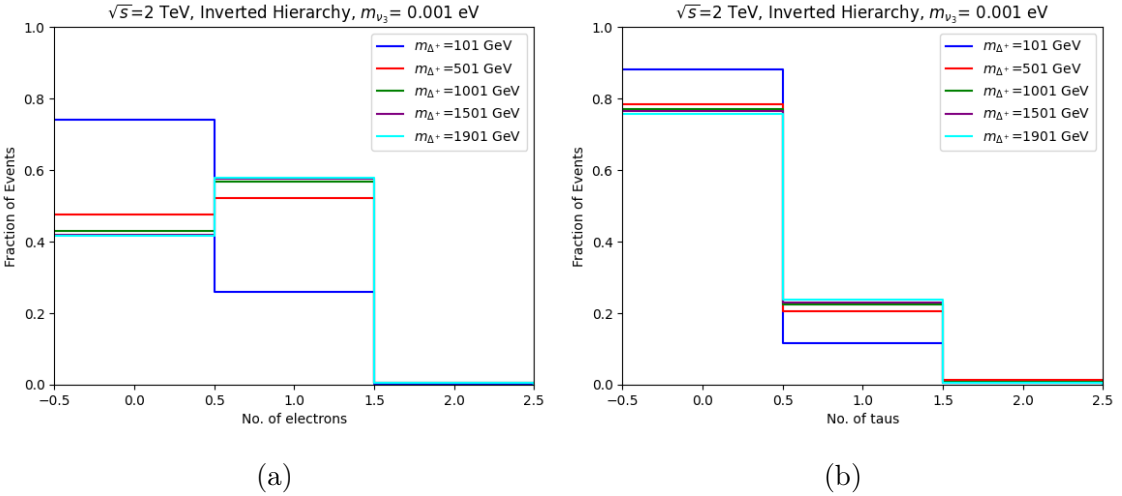


Figure 10: Distribution for a) Electrons in the final state and b) Taus in the final state for $m_{\nu_3} = 0.001 \text{ eV}$ assuming Inverted Hierarchy

beyond the scope of this work. Therefore, given the detector design as in the default muon collider delphes card, we find the limit at what mass of the lightest neutrino the difference between the hierarchies could be observed from the flavor of the final state leptons. We find that for lightest neutrino mass $\leq 0.02 \text{ eV}$, one starts to differentiate between Normal and Inverted hierarchy. We compare the distribution of Electrons and Taus for Normal and Inverted hierarchies for $m_{\nu_{lightest}} = 0.02 \text{ eV}$ and $m_{\Delta^+} = 101, 1001$ and 1901 GeV respectively in Fig. 14 - Fig. 16 where it is evident that indeed if the underlying theory respects Normal hierarchy then there will be more events with Taus in the final state and if the underlying theory respects Inverted hierarchy then there will be more events with Electrons in the final state. The same conclusion holds true for lightest neutrino mass = 0.001 eV as it is

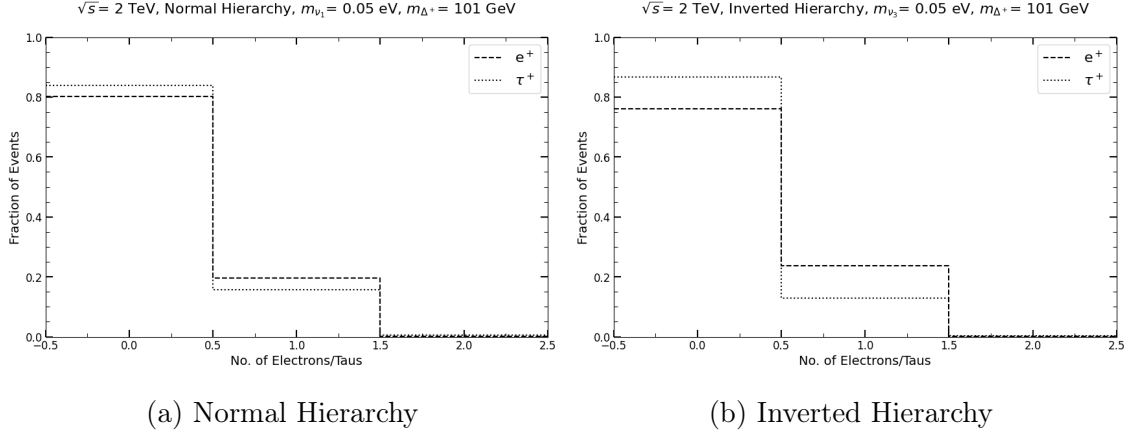


Figure 11: Distributions of Electrons and Taus for $m_{\nu_{lightest}} = 0.05$ eV and $m_{\Delta^+} = 101$ GeV assuming a) Normal Hierarchy and b) Inverted Hierarchy

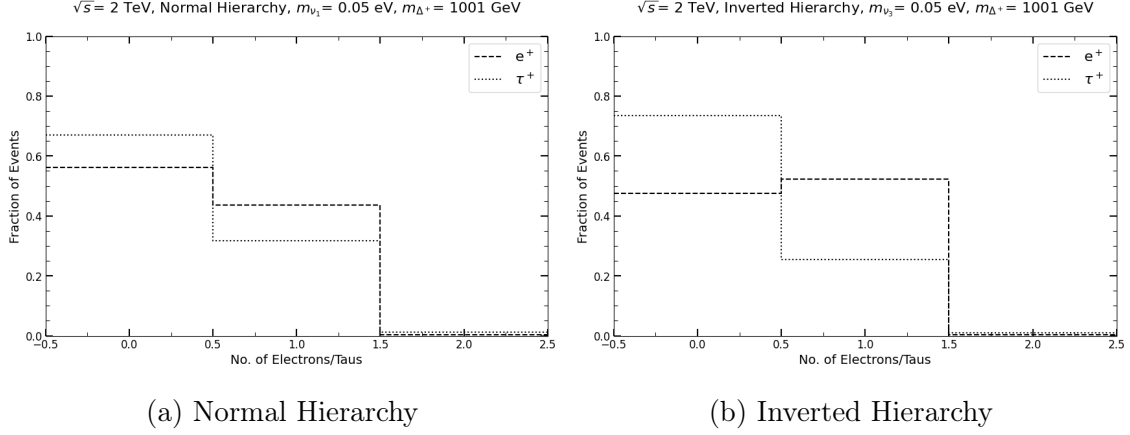


Figure 12: Distributions of Electrons and Taus for $m_{\nu_{lightest}} = 0.05$ eV and $m_{\Delta^+} = 1001$ GeV assuming a) Normal Hierarchy and b) Inverted Hierarchy

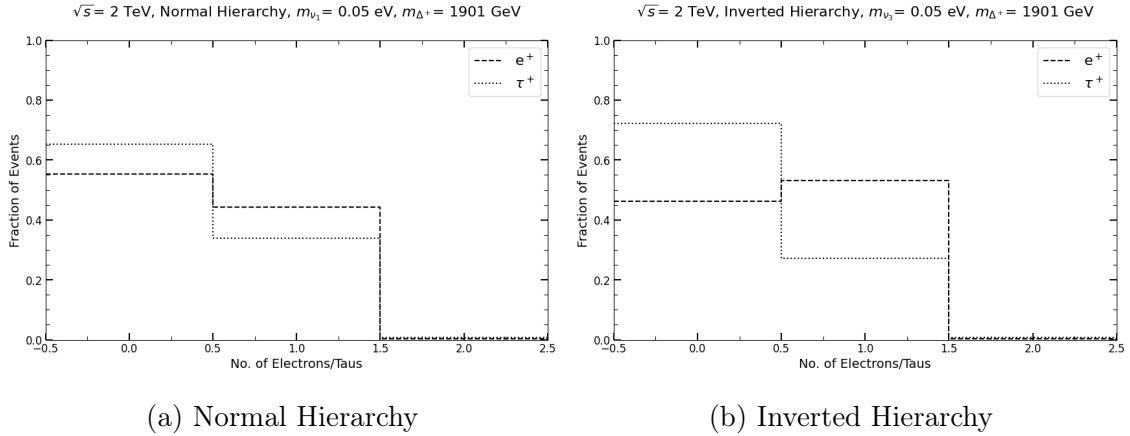


Figure 13: Distributions of Electrons and Taus for $m_{\nu_{lightest}} = 0.05$ eV and $m_{\Delta^+} = 1901$ GeV assuming a) Normal Hierarchy and b) Inverted Hierarchy

evident from Fig. 17 - Fig. 19 which compares the distribution of Electrons and Taus for

Normal and Inverted hierarchies for $m_{\nu_{lightest}} = 0.001$ eV and $m_{\Delta^+} = 101, 1001$ and 1901 GeV respectively.

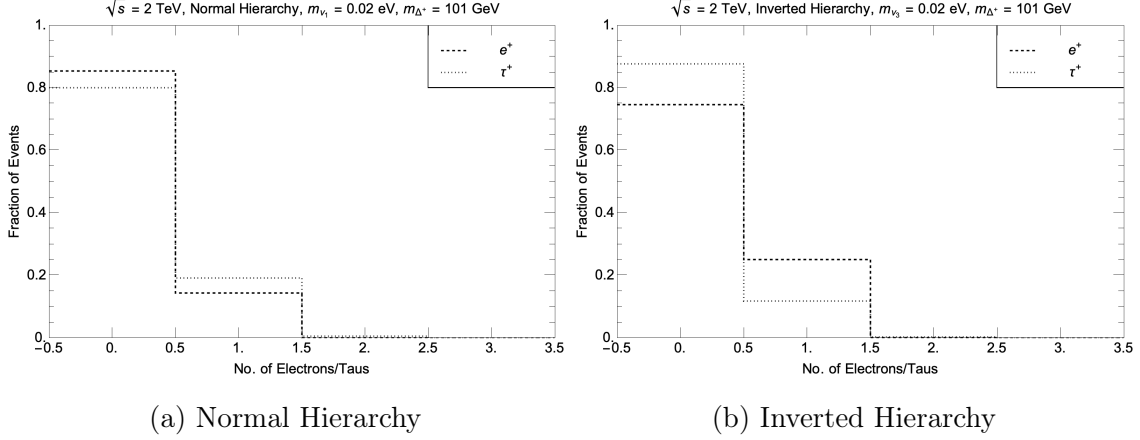


Figure 14: Distributions of Electrons and Taus for $m_{\nu_{lightest}} = 0.02$ eV and $m_{\Delta^+} = 101$ GeV assuming a) Normal Hierarchy and b) Inverted Hierarchy

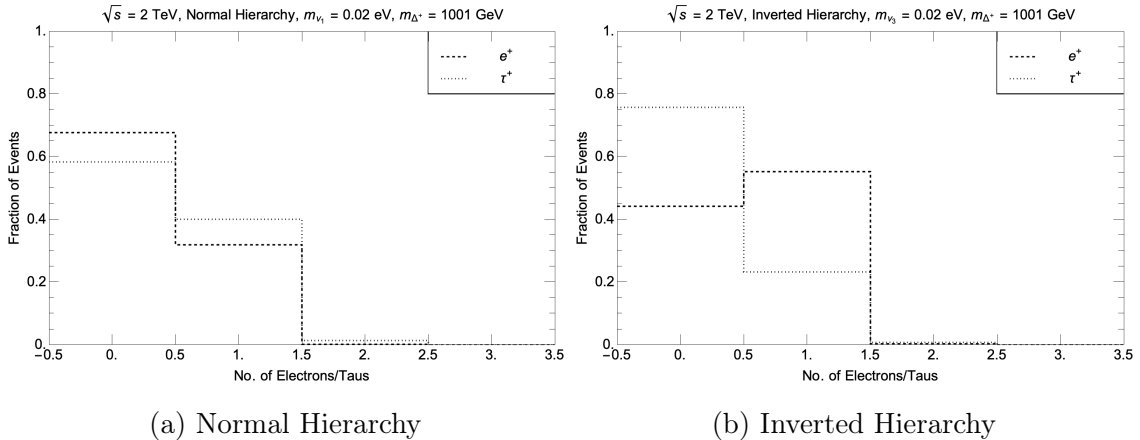


Figure 15: Distributions of Electrons and Taus for $m_{\nu_{lightest}} = 0.02$ eV and $m_{\Delta^+} = 1001$ GeV assuming a) Normal Hierarchy and b) Inverted Hierarchy

6 Summary and Outlook

Although hadron colliders such as the LHC are extremely advantageous in looking for new BSM particles produced via direct production, owing to much higher c.o.m energy as compared to the c.o.m energy in lepton colliders, a lepton collider enjoys a much cleaner environment with reduced SM background and is therefore more advantageous in looking for new BSM particles/processes involving electroweak interactions only. Additionally in lepton colliders the full c.o.m energy is used as a lepton, unlike a hadron, is a fundamental particle and hence lepton colliders offer a higher physics reach then hadron colliders for a given c.o.m

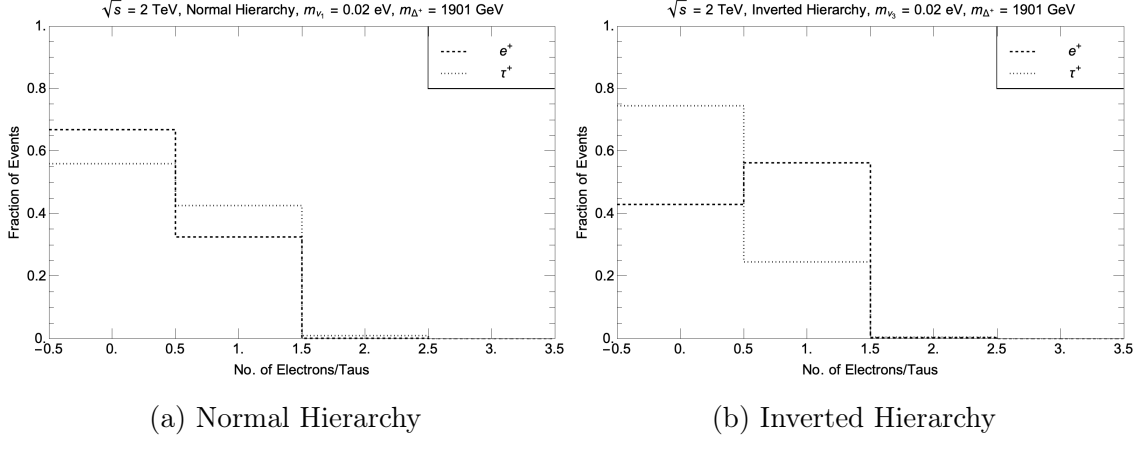


Figure 16: Distributions of Electrons and Taus for $m_{\nu_{lightest}} = 0.02 \text{ eV}$ and $m_{\Delta^+} = 1901 \text{ GeV}$ assuming a) Normal Hierarchy and b) Inverted Hierarchy

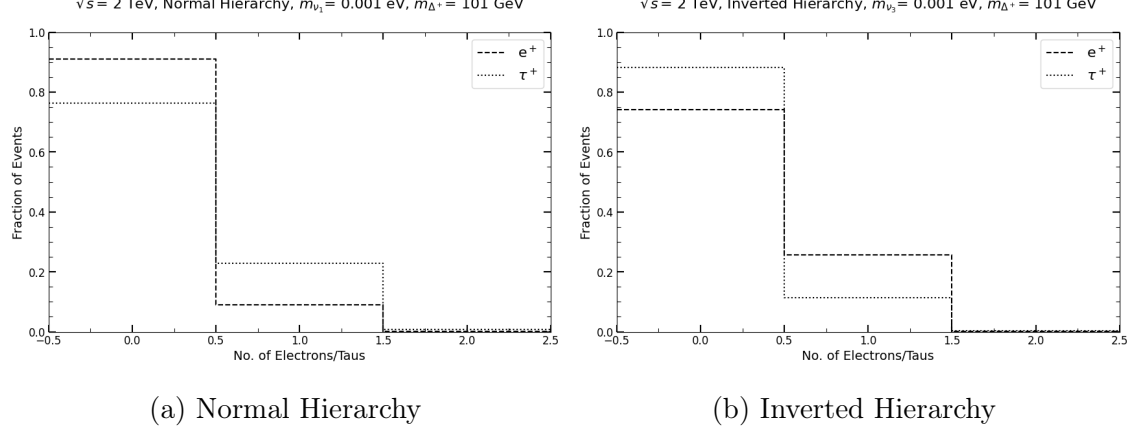


Figure 17: Distributions of Electrons and Taus for $m_{\nu_{lightest}} = 0.001 \text{ eV}$ and $m_{\Delta^+} = 101 \text{ GeV}$ assuming a) Normal Hierarchy and b) Inverted Hierarchy

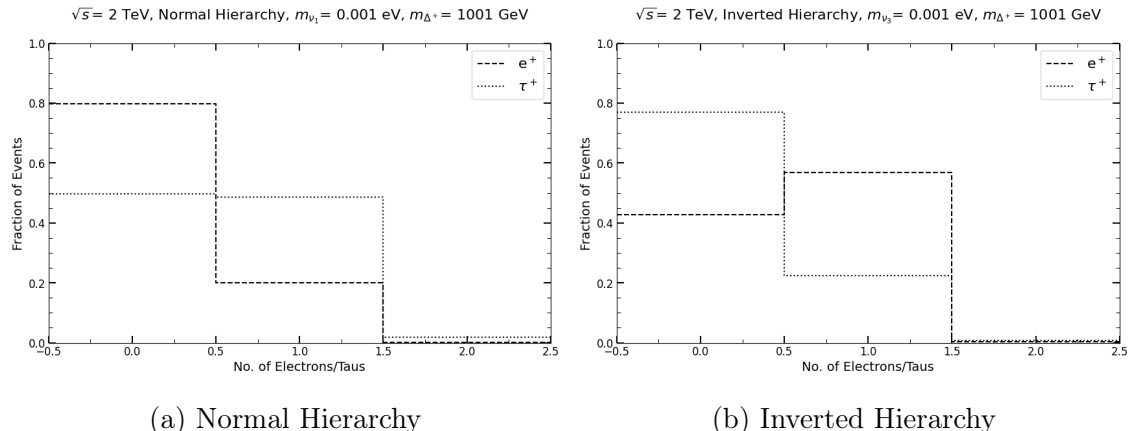


Figure 18: Distributions of Electrons and Taus for $m_{\nu_{lightest}} = 0.001 \text{ eV}$ and $m_{\Delta^+} = 1001 \text{ GeV}$ assuming a) Normal Hierarchy and b) Inverted Hierarchy

energy. Several lepton colliders such as e^+e^- collider, $\mu^+\mu^-$ collider, $\mu^+\mu^+$ collider, μ^+e^-

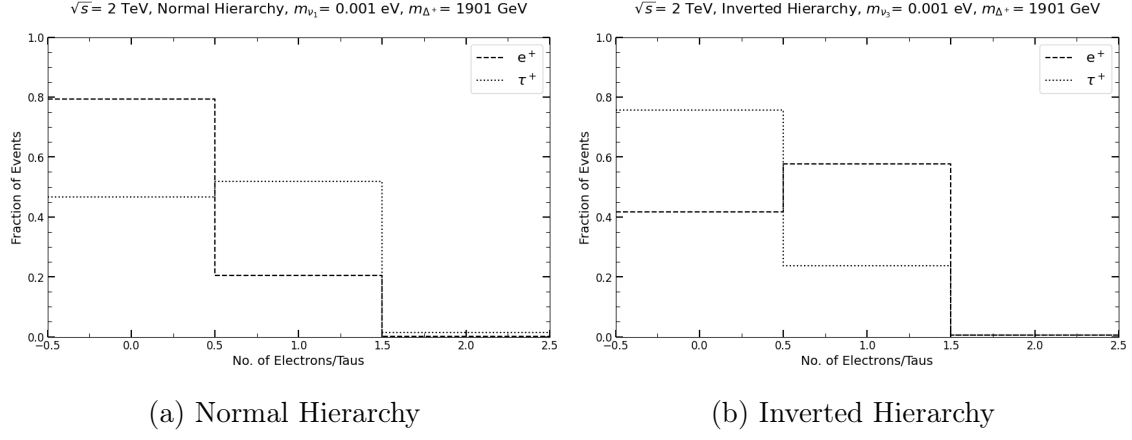


Figure 19: Distributions of Electrons and Taus for $m_{\nu_{lightest}} = 0.001$ eV and $m_{\Delta^+} = 1901$ GeV assuming a) Normal Hierarchy and b) Inverted Hierarchy

collider have been proposed to build. However, in this article we focus on the $\mu^+ \mu^+$ mode of the μ TRISTAN [26] that is planned to operate at $\sqrt{s} = 2$ TeV. The reasons behind choosing this particular setup among several proposed lepton colliders are two fold: *i*) Muon colliders lead to smaller loss of energy due to synchrotron radiations than Electron colliders as Muons are heavier than Electrons. *ii*) Building a $\mu^+ \mu^+$ collider appears to be more convenient than building a $\mu^+ \mu^-$ collider due to the cooling technology developed at J-PARC [28] which can apparently yield μ^+ more efficiently than μ^- such that they are suitable for performing collision at desired c.o.m energy. While several studies have been performed in the $\mu^+ \mu^+$ collider searching for doubly-charged scalar Δ^{++} and electrically neutral heavy scalar Δ^0 [33–36] both of which naturally occur in several BSM scenarios such as [12, 13, 15, 44–61], there hasn't been any study in search of the singly-charged scalar in the $\mu^+ \mu^+$ collider which also naturally occurs in the above-mentioned BSM scenarios. In this article we look into the discovery prospect of the singly-charged scalar at the $\mu^+ \mu^+$ collider at $\sqrt{s} = 2$ TeV in one of the above-mentioned BSM scenarios, namely, the simplest type-II seesaw scenario [12–15] which is an extremely well-motivated BSM scenario as it provides a viable mechanism for neutrino mass generation. We study the associated production of Δ^+ along with a W boson followed by the former decaying leptonically and the latter decaying hadronically. Additionally, since the type-II seesaw scenario allows for LFV processes which the SM does not, we take into consideration Δ^+ decaying into e^+ or τ^+ only as this constraint gets rid of the SM background completely which would otherwise be huge if Δ^+ decaying to μ^+ would also have been considered. On studying the signature of our choice (Fig. 2) for two benchmark points with a mass of the lightest neutrino = 0.05 eV and 0.001 eV, and m_{Δ^+} varying between 100 and 1900 GeV, we find that the $\mu^+ \mu^+$ collider operating at $\sqrt{s} = 2$ TeV is capable of yielding a cross-section with significance above 5σ for the entire mass range of Δ^+ for $m_{\nu_{lightest}} = 0.05$ eV assuming Normal or Inverted hierarchy, while for $m_{\nu_{lightest}} = 0.001$ eV, assuming Normal

hierarchy $m_{\Delta^+} \lesssim 141$ GeV and $1412 \lesssim m_{\Delta^+} \lesssim 1832$ GeV have significance above 5σ and assuming Inverted hierarchy points with $m_{\nu_{lightest}} = 0.001$ eV and $m_{\Delta^+} \lesssim 208$ GeV and $1306 \lesssim m_{\Delta^+} \lesssim 1841$ GeV have significance above 5σ . Both the benchmark points with $m_{\nu_{lightest}} = 0.05$ eV and 0.001 eV have cross-section above 95% C.L. over the complete mass range of Δ^+ from 100 to 1900 GeV. However, the cross-section or the significance plot is not sufficient to indicate whether the underlying theory respects Normal or Inverted Hierarchy since both the cases yield curves of similar shape as can be seen in Fig. 6. The negligibly small difference between the curves for Normal and Inverted hierarchy, as in Fig. 6, might vanish subject to experimental uncertainties. Therefore, in order to identify the hierarchy one must look into the distribution of the charged leptons in the final state originating from the decay of Δ^+ . As discussed in Sec. 5, Normal hierarchy leads Δ^+ to primarily decay to τ^+ while with Inverted hierarchy Δ^+ primarily decays to e^+ . However, as we see in Sec. 5, with the given detector design the distinction between the underlying hierarchies can be done only if $m_{\nu_{lightest}} \leq 0.02$ eV. With $m_{\nu_{lightest}} > 0.02$ eV, the distinction between the underlying hierarchies could be possible with some modifications in the detector design and considering other factors such as uncertainties, response function etc., which will be referred to in a related future work. Hence to conclude, the $\mu^+\mu^+$ collider running at $\sqrt{s} = 2$ TeV is an excellent tool for discovering a singly-charged scalar which can, in turn, hint towards the existence of the type-II seesaw BSM scenario. This experimental setup can also be used to distinguish between Normal and Inverted hierarchy leading to a highly important deduction regarding the underlying theory.

7 Acknowledgment

This work was partly supported by the National Science Centre, Poland, under the OPUS 27 funding scheme, project no. 2024/53/B/ST2/00975. The work of N.O. is supported in part by the United States Department of Energy Grant Nos. DE-SC0012447, DE-SC0023713, and DE-SC0026347. The work of D.S. was partly supported by the European Research Council (ERC) under the European Union’s Horizon 2020 research and innovation programme (Grant agreement No. 949451). SKV is supported by ANRF, DST, Govt. of India Grants, CRG/2021/007170 “Tiny Effects from Heavy New Physics “and REDA funds from IISc.

A Doubly-charged scalar (Δ^{++}) in Muon collider

Here we present a comparative study for pair production of the doubly-charged scalar in the Muon collider at $\sqrt{s} = 3$ TeV. The cross-sections for the lightest neutrino mass = 0.05

eV for both Normal and Inverted Hierarchy are presented in Table. III. Similar results for lightest neutrino mass = 0.001 eV is presented in Table. IV

Masses [GeV]			Normal Hierarchy				Inverted Hierarchy			
m_{Δ^0}	m_{Δ^+}	$m_{\Delta^{++}}$	Γ_{Δ^0}	Γ_{Δ^+}	$\Gamma_{\Delta^{++}}$	σ	Γ_{Δ^0}	Γ_{Δ^+}	$\Gamma_{\Delta^{++}}$	σ
100	101	103	0.02	0.0202	0.0206	0.0123	0.0247	0.0249	0.0254	0.01236
300	301	303	0.0601	0.0603	0.0607	0.01155	0.0742	0.0744	0.0749	0.01162
500	501	503	0.1002	0.1004	0.1008	0.01025	0.1236	0.1239	0.1243	0.01032
1000	1001	1003	0.2004	0.2006	0.201	0.005	0.2472	0.2475	0.248	0.005022

Table III: Benchmark Points for Normal and Inverted Hierarchy at $v_{\Delta} = 10^{-9}$ GeV and lightest neutrino mass = 0.05 eV. The cross-section listed here is for the process $\mu^+\mu^- > \Delta^{++}\Delta^{--}$ at $\sqrt{s} = 3$ TeV. All the masses and decay widths(Γ) are in units of GeV and the cross-sections σ are in units of pb.

Masses [GeV]			Normal Hierarchy				Inverted Hierarchy			
m_{Δ^0}	m_{Δ^+}	$m_{\Delta^{++}}$	Γ_{Δ^0}	Γ_{Δ^+}	$\Gamma_{\Delta^{++}}$	σ	Γ_{Δ^0}	Γ_{Δ^+}	$\Gamma_{\Delta^{++}}$	σ
100	101	103	$5.13 \cdot 10^{-3}$	$5.18 \cdot 10^{-3}$	$5.28 \cdot 10^{-3}$	0.01275	$9.806 \cdot 10^{-3}$	$9.902 \cdot 10^{-3}$	$1.01 \cdot 10^{-2}$	0.01284
300	301	303	$1.538 \cdot 10^{-2}$	$1.543 \cdot 10^{-2}$	$1.553 \cdot 10^{-2}$	0.01205	$2.942 \cdot 10^{-2}$	$2.952 \cdot 10^{-2}$	$2.971 \cdot 10^{-2}$	0.01214
500	501	503	$2.563 \cdot 10^{-2}$	$2.568 \cdot 10^{-2}$	$2.58 \cdot 10^{-2}$	0.01071	$4.903 \cdot 10^{-2}$	$4.913 \cdot 10^{-2}$	$4.932 \cdot 10^{-2}$	0.01078
1000	1001	1003	$5.126 \cdot 10^{-2}$	$5.132 \cdot 10^{-2}$	$5.142 \cdot 10^{-2}$	0.005246	$9.806 \cdot 10^{-2}$	$9.816 \cdot 10^{-2}$	$9.836 \cdot 10^{-2}$	0.005289

Table IV: Benchmark Points for Normal and Inverted Hierarchy at $v_{\Delta} = 10^{-9}$ GeV and lightest neutrino mass = 0.001 eV. The cross-section listed here is for the process $\mu^+\mu^- > \Delta^{++}\Delta^{--}$ at $\sqrt{s} = 3$ TeV. All the masses and decay widths(Γ) are in units of GeV and the cross-sections σ are in units of pb.

B Doubly-charged scalar (Δ^{++}) in $\mu^+\mu^+$ mode of μ TRISTAN

This section shows another comparative study for production of the doubly-charged scalar in the μ TRISTAN at $\sqrt{s} = 2$ TeV. The cross-sections for the lightest neutrino mass = 0.05 eV for both Normal and Inverted Hierarchy are presented in Table. V. Similar results for lightest neutrino mass = 0.001 eV is presented in Table. VI

Masses [GeV]			Normal Hierarchy				Inverted Hierarchy			
m_{Δ^0}	m_{Δ^+}	$m_{\Delta^{++}}$	Γ_{Δ^0}	Γ_{Δ^+}	$\Gamma_{\Delta^{++}}$	σ	Γ_{Δ^0}	Γ_{Δ^+}	$\Gamma_{\Delta^{++}}$	σ
100	101	103	0.02	0.0202	0.0206	$1.419 \cdot 10^{-5}$	0.0247	0.0249	0.0254	$1.146 \cdot 10^{-5}$
300	301	303	0.0601	0.0603	0.0607	$1.478 \cdot 10^{-5}$	0.0742	0.0744	0.0749	$1.194 \cdot 10^{-5}$
500	501	503	0.1002	0.1004	0.1008	$1.608 \cdot 10^{-5}$	0.1236	0.1239	0.1243	$1.299 \cdot 10^{-5}$
1000	1001	1003	0.2004	0.2006	0.201	$2.519 \cdot 10^{-5}$	0.2472	0.2475	0.248	$2.035 \cdot 10^{-5}$
1500	1501	1503	0.3006	0.3008	0.3012	$7.448 \cdot 10^{-5}$	0.3708	0.3711	0.3716	$6.018 \cdot 10^{-5}$
1900	1901	1903	0.3808	0.381	0.3814	0.001575	0.4697	0.47	0.4704	$1.273 \cdot 10^{-3}$

Table V: Benchmark Points for Normal and Inverted Hierarchy at $v_\Delta = 10^{-9}$ GeV and lightest neutrino mass = 0.05 eV. The cross-section listed here is for the process $\mu^+\mu^+ > \Delta^{++} > \mu^+\mu^+$ at $\sqrt{s} = 2$ TeV. All the masses and decay widths(Γ) are in units of GeV and the cross-sections σ are in units of pb.

Masses [GeV]			Normal Hierarchy				Inverted Hierarchy			
m_{Δ^0}	m_{Δ^+}	$m_{\Delta^{++}}$	Γ_{Δ^0}	Γ_{Δ^+}	$\Gamma_{\Delta^{++}}$	σ	Γ_{Δ^0}	Γ_{Δ^+}	$\Gamma_{\Delta^{++}}$	σ
100	101	103	$5.13 \cdot 10^{-3}$	$5.18 \cdot 10^{-3}$	$5.28 \cdot 10^{-3}$	$8.531 \cdot 10^{-7}$	$9.806 \cdot 10^{-3}$	$9.902 \cdot 10^{-3}$	$1.01 \cdot 10^{-2}$	$2.195 \cdot 10^{-7}$
300	301	303	$1.538 \cdot 10^{-2}$	$1.543 \cdot 10^{-2}$	$1.553 \cdot 10^{-2}$	$8.889 \cdot 10^{-7}$	$2.942 \cdot 10^{-2}$	$2.952 \cdot 10^{-2}$	$2.971 \cdot 10^{-2}$	$2.287 \cdot 10^{-7}$
500	501	503	$2.563 \cdot 10^{-2}$	$2.568 \cdot 10^{-2}$	$2.58 \cdot 10^{-2}$	$9.67 \cdot 10^{-7}$	$4.903 \cdot 10^{-2}$	$4.913 \cdot 10^{-2}$	$4.932 \cdot 10^{-2}$	$2.488 \cdot 10^{-7}$
1000	1001	1003	$5.126 \cdot 10^{-2}$	$5.132 \cdot 10^{-2}$	$5.142 \cdot 10^{-2}$	$1.515 \cdot 10^{-6}$	$9.806 \cdot 10^{-2}$	$9.816 \cdot 10^{-2}$	$9.836 \cdot 10^{-2}$	$3.897 \cdot 10^{-7}$
1500	1501	1503	$7.69 \cdot 10^{-2}$	$7.695 \cdot 10^{-2}$	$7.705 \cdot 10^{-2}$	$4.479 \cdot 10^{-6}$	$1.471 \cdot 10^{-1}$	$1.472 \cdot 10^{-1}$	$1.474 \cdot 10^{-1}$	$1.153 \cdot 10^{-6}$
1900	1901	1903	$9.741 \cdot 10^{-2}$	$9.746 \cdot 10^{-2}$	$9.756 \cdot 10^{-2}$	$9.472 \cdot 10^{-5}$	$1.863 \cdot 10^{-1}$	$1.864 \cdot 10^{-1}$	$1.866 \cdot 10^{-1}$	$2.437 \cdot 10^{-5}$

Table VI: Benchmark Points for Normal and Inverted Hierarchy at $v_\Delta = 10^{-9}$ GeV and lightest neutrino mass = 0.001 eV. The cross-section listed here is for the process $\mu^+\mu^+ > \Delta^{++} > \mu^+\mu^+$ at $\sqrt{s} = 2$ TeV. All the masses and decay widths(Γ) are in units of GeV and the cross-sections σ are in units of pb.

C Analytical formula for the signal process

This section explains the fall and rise nature of the curve obtained in Fig. 3 for cross-section of our signature of interest. For the processes (a) and (b) shown in Fig. 2, the corresponding helicity amplitudes $\mathcal{M}_{(a)}(s_1, s_2, s_3)$ and $\mathcal{M}_{(b)}(s_1, s_2, s_3)$ are given as follows. Here, $s_1 = \pm$, $s_2 = \pm$ are the helicities of the initial anti-Muons, and $s_3 = \pm, 0$ is the helicity of the final state W boson.

$$\begin{aligned} \mathcal{M}_{(a)}(-, -, 0)/Y_{\mu\mu}^* &= -\mathcal{M}_{(a)}(+, +, 0)/Y_{\mu\mu}^* \\ &= -\frac{\sqrt{2}\sqrt{s}\sqrt{(s - m_\Delta^2 - m_W^2)^2 - 4m_\Delta^2m_W^2}}{m_W(s - m_\Delta^2)}. \end{aligned} \quad (\text{C.10})$$

$$\begin{aligned} \mathcal{M}_{(b)}(-, -, \mp)/Y_{\mu\mu}^* &= -\mathcal{M}_{(b)}(+, +, \pm)/Y_{\mu\mu}^* \\ &= \frac{\sin\theta}{2} \frac{s - m_W^2 + m_\Delta^2 \pm \sqrt{(s - m_\Delta^2 - m_W^2)^2 - 4m_\Delta^2m_W^2}}{s - m_W^2 - m_\Delta^2 - \cos\theta\sqrt{(s - m_\Delta^2 - m_W^2)^2 - 4m_\Delta^2m_W^2}} \\ &- \frac{\sin\theta}{2} \frac{s - m_W^2 + m_\Delta^2 \pm \sqrt{(s - m_\Delta^2 - m_W^2)^2 - 4m_\Delta^2m_W^2}}{s - m_W^2 - m_\Delta^2 + \cos\theta\sqrt{(s - m_\Delta^2 - m_W^2)^2 - 4m_\Delta^2m_W^2}} \end{aligned} \quad (\text{C.11})$$

$$\begin{aligned} \mathcal{M}_{(b)}(-, -, 0)/Y_{\mu\mu}^* &= -\mathcal{M}_{(b)}(+, +, 0)/Y_{\mu\mu}^* \\ &= \frac{\sqrt{s} \left(\sqrt{(s + m_W^2 - m_\Delta^2)^2 - 4m_\Delta^2m_W^2} - \cos\theta(s - m_\Delta^2 - m_W^2) \right)}{\sqrt{2}m_W \left(s - m_\Delta^2 - m_W^2 - \cos\theta\sqrt{(s - m_\Delta^2 - m_W^2)^2 - 4m_\Delta^2m_W^2} \right)} \\ &+ \frac{\sqrt{s} \left(\sqrt{(s + m_W^2 - m_\Delta^2)^2 - 4m_\Delta^2m_W^2} + \cos\theta(s - m_\Delta^2 - m_W^2) \right)}{\sqrt{2}m_W \left(s - m_\Delta^2 - m_W^2 + \cos\theta\sqrt{(s - m_\Delta^2 - m_W^2)^2 - 4m_\Delta^2m_W^2} \right)} \end{aligned} \quad (\text{C.12})$$

Other helicity combinations are all zero. For the process (b), we have neglected the ν_ℓ masses. The cross-term between $\mathcal{M}_{(a)}(\pm, \pm, 0)$ and $\mathcal{M}_{(b)}(\pm, \pm, 0)$ yields destructive interference that first decreases and then increases with increasing m_Δ . This fall and rise behaviour of the destructive interference term explains the typical fall and rise nature of the curves with increasing m_Δ as seen in Fig. 3 and Fig. 6.

References

- [1] **ATLAS** Collaboration, G. Aad *et al.*, “Observation of a new particle in the search for the Standard model Higgs boson with the ATLAS detector at the LHC,” *Phys. Lett. B* **716** (2012) 1–29, [arXiv:1207.7214 \[hep-ex\]](https://arxiv.org/abs/1207.7214).
- [2] **CMS** Collaboration, S. Chatrchyan *et al.*, “Observation of a New Boson at a Mass of 125 GeV with the CMS Experiment at the LHC,” *Phys. Lett. B* **716** (2012) 30–61, [arXiv:1207.7235 \[hep-ex\]](https://arxiv.org/abs/1207.7235).

- [3] R. N. Mohapatra and A. Y. Smirnov, “Neutrino Mass and New Physics,” *Ann. Rev. Nucl. Part. Sci.* **56** (2006) 569–628, [arXiv:hep-ph/0603118](https://arxiv.org/abs/hep-ph/0603118).
- [4] A. de Gouv  a, “Neutrino Mass Models,” *Ann. Rev. Nucl. Part. Sci.* **66** (2016) 197–217.
- [5] V. Branchina and E. Messina, “Stability, Higgs Boson Mass and New Physics,” *Phys. Rev. Lett.* **111** (2013) 241801, [arXiv:1307.5193 \[hep-ph\]](https://arxiv.org/abs/1307.5193).
- [6] L. Susskind, “Dynamics of Spontaneous Symmetry Breaking in the Weinberg-Salam Theory,” *Phys. Rev. D* **20** (1979) 2619–2625.
- [7] M. J. G. Veltman, “The Infrared - Ultraviolet Connection,” *Acta Phys. Polon. B* **12** (1981) 437.
- [8] A. D. Sakharov, “Violation of CP Invariance, C asymmetry, and baryon asymmetry of the universe,” *Pisma Zh. Eksp. Teor. Fiz.* **5** (1967) 32–35.
- [9] R. D. Peccei and H. R. Quinn, “Some Aspects of Instantons,” *Nuovo Cim. A* **41** (1977) 309.
- [10] R. D. Peccei and H. R. Quinn, “CP Conservation in the Presence of Instantons,” *Phys. Rev. Lett.* **38** (1977) 1440–1443.
- [11] R. D. Peccei and H. R. Quinn, “Constraints Imposed by CP Conservation in the Presence of Instantons,” *Phys. Rev. D* **16** (1977) 1791–1797.
- [12] M. Magg and C. Wetterich, “Neutrino Mass Problem and Gauge Hierarchy,” *Phys. Lett. B* **94** (1980) 61–64.
- [13] J. Schechter and J. W. F. Valle, “Neutrino Masses in SU(2) x U(1) Theories,” *Phys. Rev. D* **22** (1980) 2227.
- [14] R. N. Mohapatra and G. Senjanovic, “Neutrino Mass and Spontaneous Parity Nonconservation,” *Phys. Rev. Lett.* **44** (1980) 912.
- [15] G. Lazarides, Q. Shafi, and C. Wetterich, “Proton Lifetime and Fermion Masses in an SO(10) Model,” *Nucl. Phys. B* **181** (1981) 287–300.
- [16] F. F. Deppisch, P. S. Bhupal Dev, and A. Pilaftsis, “Neutrinos and Collider Physics,” *New J. Phys.* **17** no. 7, (2015) 075019, [arXiv:1502.06541 \[hep-ph\]](https://arxiv.org/abs/1502.06541).
- [17] Y. Cai, T. Han, T. Li, and R. Ruiz, “Lepton Number Violation: Seesaw Models and Their Collider Tests,” *Front. in Phys.* **6** (2018) 40, [arXiv:1711.02180 \[hep-ph\]](https://arxiv.org/abs/1711.02180).

[18] L. Calibbi and G. Signorelli, “Charged Lepton Flavour Violation: An Experimental and Theoretical Introduction,” *Riv. Nuovo Cim.* **41** no. 2, (2018) 71–174, [arXiv:1709.00294 \[hep-ph\]](https://arxiv.org/abs/1709.00294).

[19] S. Davidson, B. Echenard, R. H. Bernstein, J. Heeck, and D. G. Hitlin, “Charged Lepton Flavor Violation,” [arXiv:2209.00142 \[hep-ex\]](https://arxiv.org/abs/2209.00142).

[20] J. P. Delahaye, M. Diemoz, K. Long, B. Mansoulié, N. Pastrone, L. Rivkin, D. Schulte, A. Skrinsky, and A. Wulzer, “Muon Colliders,” [arXiv:1901.06150 \[physics.acc-ph\]](https://arxiv.org/abs/1901.06150).

[21] K. Long, D. Lucchesi, M. Palmer, N. Pastrone, D. Schulte, and V. Shiltsev, “Muon colliders to expand frontiers of particle physics,” *Nature Phys.* **17** no. 3, (2021) 289–292, [arXiv:2007.15684 \[physics.acc-ph\]](https://arxiv.org/abs/2007.15684).

[22] H. Al Ali *et al.*, “The muon Smasher’s guide,” *Rept. Prog. Phys.* **85** no. 8, (2022) 084201, [arXiv:2103.14043 \[hep-ph\]](https://arxiv.org/abs/2103.14043).

[23] **Muon Collider** Collaboration, J. de Blas *et al.*, “The physics case of a 3 TeV muon collider stage,” [arXiv:2203.07261 \[hep-ph\]](https://arxiv.org/abs/2203.07261).

[24] C. Accettura *et al.*, “Towards a muon collider,” *Eur. Phys. J. C* **83** no. 9, (2023) 864, [arXiv:2303.08533 \[physics.acc-ph\]](https://arxiv.org/abs/2303.08533). [Erratum: Eur.Phys.J.C 84, 36 (2024)].

[25] C. Aime *et al.*, “Muon Collider Physics Summary,” [arXiv:2203.07256 \[hep-ph\]](https://arxiv.org/abs/2203.07256).

[26] Y. Hamada, R. Kitano, R. Matsudo, H. Takaura, and M. Yoshida, “ μ TRISTAN,” *PTEP* **2022** no. 5, (2022) 053B02, [arXiv:2201.06664 \[hep-ph\]](https://arxiv.org/abs/2201.06664).

[27] C. A. Heusch and F. Cuypers, “Physics with like-sign muon beams in a TeV muon collider,” *AIP Conf. Proc.* **352** (1996) 219–231, [arXiv:hep-ph/9508230](https://arxiv.org/abs/hep-ph/9508230).

[28] M. Abe *et al.*, “A New Approach for Measuring the Muon Anomalous Magnetic Moment and Electric Dipole Moment,” *PTEP* **2019** no. 5, (2019) 053C02, [arXiv:1901.03047 \[physics.ins-det\]](https://arxiv.org/abs/1901.03047).

[29] F. Bossi and P. Ciafaloni, “Lepton Flavor Violation at muon-electron colliders,” *JHEP* **10** (2020) 033, [arXiv:2003.03997 \[hep-ph\]](https://arxiv.org/abs/2003.03997).

[30] M. Lu, A. M. Levin, C. Li, A. Agapitos, Q. Li, F. Meng, S. Qian, J. Xiao, and T. Yang, “The physics case for an electron-muon collider,” *Adv. High Energy Phys.* **2021** (2021) 6693618, [arXiv:2010.15144 \[hep-ph\]](https://arxiv.org/abs/2010.15144).

[31] G. Lichtenstein, M. A. Schmidt, G. Valencia, and R. R. Volkas, “Complementarity of μ TRISTAN and Belle II in searches for charged-lepton flavour violation,” *Phys. Lett. B* **845** (2023) 138144, [arXiv:2307.11369 \[hep-ph\]](https://arxiv.org/abs/2307.11369).

[32] A. Das, T. Nomura, and T. Shimomura, “Multi muon/anti-muon signals via productions of gauge and scalar bosons in a $U(1)_{L_\mu - L_\tau}$ model at muonic colliders,” *Eur. Phys. J. C* **83** no. 9, (2023) 786, [arXiv:2212.11674 \[hep-ph\]](https://arxiv.org/abs/2212.11674).

[33] J.-L. Yang, C.-H. Chang, and T.-F. Feng, “Leptonic di-flavor and di-number violation processes at high energy colliders*,” *Chin. Phys. C* **48** no. 4, (2024) 043101, [arXiv:2302.13247 \[hep-ph\]](https://arxiv.org/abs/2302.13247).

[34] K. Fridell, R. Kitano, and R. Takai, “Lepton flavor physics at $\mu^+ \mu^+$ colliders,” *JHEP* **06** (2023) 086, [arXiv:2304.14020 \[hep-ph\]](https://arxiv.org/abs/2304.14020).

[35] P. S. B. Dev, J. Heeck, and A. Thapa, “Neutrino mass models at μ TRISTAN,” *Eur. Phys. J. C* **84** no. 2, (2024) 148, [arXiv:2309.06463 \[hep-ph\]](https://arxiv.org/abs/2309.06463).

[36] J.-C. Jia, Z.-L. Han, F. Huang, Y. Jin, and H. Li, “Production of single doubly charged Higgs bosons at muon colliders,” *Phys. Rev. D* **111** no. 1, (2025) 015009, [arXiv:2409.16582 \[hep-ph\]](https://arxiv.org/abs/2409.16582).

[37] R. Kitano, I. Low, R. Matsudo, S. Okawa, and S. Roy, “Heavy Neutral Lepton at Same-Sign Muon Collider,” [arXiv:2510.18390 \[hep-ph\]](https://arxiv.org/abs/2510.18390).

[38] **Particle Data Group** Collaboration, P. A. Zyla *et al.*, “Review of Particle Physics,” *PTEP* **2020** no. 8, (2020) 083C01.

[39] N. Ghosh, S. K. Rai, T. Samui, and A. Sarkar, “Investigating the leptonic couplings of doubly charged scalars at the muon collider,” [arXiv:2506.00966 \[hep-ph\]](https://arxiv.org/abs/2506.00966).

[40] B. Fuks, M. Nemevšek, and R. Ruiz, “Doubly Charged Higgs Boson Production at Hadron Colliders,” *Phys. Rev. D* **101** no. 7, (2020) 075022, [arXiv:1912.08975 \[hep-ph\]](https://arxiv.org/abs/1912.08975).

[41] J. Alwall, M. Herquet, F. Maltoni, O. Mattelaer, and T. Stelzer, “MadGraph 5 : Going Beyond,” *JHEP* **06** (2011) 128, [arXiv:1106.0522 \[hep-ph\]](https://arxiv.org/abs/1106.0522).

[42] T. Sjöstrand, S. Ask, J. R. Christiansen, R. Corke, N. Desai, P. Ilten, S. Mrenna, S. Prestel, C. O. Rasmussen, and P. Z. Skands, “An introduction to PYTHIA 8.2,” *Comput. Phys. Commun.* **191** (2015) 159–177, [arXiv:1410.3012 \[hep-ph\]](https://arxiv.org/abs/1410.3012).

[43] **DELPHES 3** Collaboration, J. de Favereau, C. Delaere, P. Demin, A. Giammanco, V. Lemaître, A. Mertens, and M. Selvaggi, “DELPHES 3, A modular framework for fast simulation of a generic collider experiment,” *JHEP* **02** (2014) 057, [arXiv:1307.6346 \[hep-ex\]](https://arxiv.org/abs/1307.6346).

[44] R. N. Mohapatra and G. Senjanovic, “Neutrino Masses and Mixings in Gauge Models with Spontaneous Parity Violation,” *Phys. Rev. D* **23** (1981) 165.

[45] J. C. Pati and A. Salam, “Lepton Number as the Fourth Color,” *Phys. Rev. D* **10** (1974) 275–289. [Erratum: Phys.Rev.D 11, 703–703 (1975)].

[46] R. N. Mohapatra and J. C. Pati, “Left-Right Gauge Symmetry and an Isoconjugate Model of CP Violation,” *Phys. Rev. D* **11** (1975) 566–571.

[47] G. Senjanovic and R. N. Mohapatra, “Exact Left-Right Symmetry and Spontaneous Violation of Parity,” *Phys. Rev. D* **12** (1975) 1502.

[48] R. Kuchimanchi and R. N. Mohapatra, “No parity violation without R-parity violation,” *Phys. Rev. D* **48** (1993) 4352–4360, [arXiv:hep-ph/9306290](https://arxiv.org/abs/hep-ph/9306290).

[49] K. S. Babu and R. N. Mohapatra, “Minimal Supersymmetric Left-Right Model,” *Phys. Lett. B* **668** (2008) 404–409, [arXiv:0807.0481 \[hep-ph\]](https://arxiv.org/abs/0807.0481).

[50] K. S. Babu and A. Patra, “Higgs Boson Spectra in Supersymmetric Left-Right Models,” *Phys. Rev. D* **93** no. 5, (2016) 055030, [arXiv:1412.8714 \[hep-ph\]](https://arxiv.org/abs/1412.8714).

[51] L. Basso, B. Fuks, M. E. Krauss, and W. Porod, “Doubly-charged Higgs and vacuum stability in left-right supersymmetry,” *JHEP* **07** (2015) 147, [arXiv:1503.08211 \[hep-ph\]](https://arxiv.org/abs/1503.08211).

[52] A. Zee, “Quantum Numbers of Majorana Neutrino Masses,” *Nucl. Phys. B* **264** (1986) 99–110.

[53] K. S. Babu, “Model of ‘Calculable’ Majorana Neutrino Masses,” *Phys. Lett. B* **203** (1988) 132–136.

[54] N. Arkani-Hamed, A. G. Cohen, E. Katz, A. E. Nelson, T. Gregoire, and J. G. Wacker, “The Minimal moose for a little Higgs,” *JHEP* **08** (2002) 021, [arXiv:hep-ph/0206020](https://arxiv.org/abs/hep-ph/0206020).

[55] K. S. Babu, P. S. B. Dev, S. Jana, and A. Thapa, “Unified framework for B -anomalies, muon $g - 2$ and neutrino masses,” *JHEP* **03** (2021) 179, [arXiv:2009.01771 \[hep-ph\]](https://arxiv.org/abs/2009.01771).

[56] H. Georgi and M. Machacek, “DOUBLY CHARGED HIGGS BOSONS,” *Nucl. Phys. B* **262** (1985) 463–477.

[57] J. F. Gunion, R. Vega, and J. Wudka, “Higgs triplets in the standard model,” *Phys. Rev. D* **42** (1990) 1673–1691.

[58] K. S. Babu, S. Nandi, and Z. Tavartkiladze, “New Mechanism for Neutrino Mass Generation and Triply Charged Higgs Bosons at the LHC,” *Phys. Rev. D* **80** (2009) 071702, [arXiv:0905.2710 \[hep-ph\]](https://arxiv.org/abs/0905.2710).

[59] F. Bonnet, D. Hernandez, T. Ota, and W. Winter, “Neutrino masses from higher than $d=5$ effective operators,” *JHEP* **10** (2009) 076, [arXiv:0907.3143 \[hep-ph\]](https://arxiv.org/abs/0907.3143).

[60] S. Bhattacharya, S. Jana, and S. Nandi, “Neutrino Masses and Scalar Singlet Dark Matter,” *Phys. Rev. D* **95** no. 5, (2017) 055003, [arXiv:1609.03274 \[hep-ph\]](https://arxiv.org/abs/1609.03274).

[61] K. Kumericki, I. Picek, and B. Radovcic, “TeV-scale Seesaw with Quintuplet Fermions,” *Phys. Rev. D* **86** (2012) 013006, [arXiv:1204.6599 \[hep-ph\]](https://arxiv.org/abs/1204.6599).